Nonequilibrium Thermodynamic Theory for Concentration Profiles in Liquid Extraction

ALPHONSE HENNICO and THEODORE VERMEULEN

University of California, Berkeley, California

The pattern or profile of concentration change in each of the two countercurrent streams, within a packed extraction column involving a three-component system, is generally assumed to follow either branch of the mutual-solubility curve for the system. In the work reported here such concentration profiles have been computed for an idealized extraction. The results show that the raffinate will usually be carried into a metastable condition inside the equilibrium curve, but the extract composition remains appreciably outside the equilibrium curve.

In the calculations mass transfer coefficient ratios are held constant at any one steady state condition of operation (called a *run*), but are varied in different runs, in order to determine the direction and magnitude of their effects. A modified activity-gradient, derived both for molecular diffusion and for penetration-theory conditions, is postulated to govern mass transfer and is used in place of the usual concentration driving potential. Solute depletion, mainly, is found to explain the result for the raffinate phase in much the same way that temperature lowering leads to supersaturation in binary solutions. Solute enrichment is the cause of the extract-phase behavior.

For ternary liquid systems undergoing countercurrent extraction in packed columns or other nonstaged equipment, calculation of the separation desired or obtained is often based upon the assumption that the composition of each coexisting phase lies on the mutual-solubility curve (*26, 29*). By contrast, certain studies of mass transfer rates between immiscible phases in binary systems have dealt entirely with the observable incompleteness of saturation in such systems, compared with the condition of equilibrium (*4, 21*). It is also well known that in binary and multicomponent systems a metastable range of compositions exists inside and adjacent to the mutual-solubility values, where nucleation will not occur spontaneously (*8, 10, 19, 20, 24, 25*). In this metastable region diffusion to a second phase is believed to provide the sole mechanism by which the system can tend toward equilibrium. Thus it is possible, in principle, to encounter nonequilibrium compositions that may lie either inside or outside the equilibrium solubility curve.

This paper examines the pattern of deviations from the mutual-solubility curve to assess the validity of the usual calculations and to see how the deviations can be related to the mass transfer coefficients for the individual components. It is assumed that the concentrations vary continuously from point to point, as in a packed column; that no longitudinal dispersion occurs, although this effect would not upset the qualitative conclusions that are found to apply in its absence; and that diffusion in the ternary mixture can be described effectively by the relations derived for binary solutions.

The results obtained, which depend upon standard approaches to thermodynamics and to mass transfer, indicate in some cases that the concentration profile can penetrate into the metastable range, in other words that equilibrium is approached from the metastable side rather than from the ordinarily stable side. This conclusion, although plausible and consistent with existing knowledge of phase equilibrium and mass transfer, has not been tested experimentally. To do so will require extremely accurate measurements; work in progress is being directed toward this objective.

THERMODYNAMIC BACKGROUND

In a two-phase liquid nonelectrolyte system the thermodynamic activity of each component, in either phase, is customarily expressed as a fraction of the activity of the corresponding pure component. Equilibrium is the condition in which the activity of each component is the same in both phases, corresponding to tie-line composition values whose locus forms the mutual-solubility curve. Figure 1 for a ternary system shows a set of activity contours, for the three components, which participate in two (matching) three-way intersections and thus define the ends of an equilibrium tie-line.*

Equations

Conclusions of a general type are sought in this investigation that will be independent of the particular calculation methods used. In order to obtain the greatest self-consistency the ternary system to be treated is defined mathematically rather than by experiment. The generality of the results is not reduced if one uses the simplest (two-suffix) equations for activity coefficients; these are contained, for instance, in Wohl's equations for ternary systems (*31*). In this treatment for component A in a ternary mixture ABC the activity-coefficient relation becomes

$$\ln \gamma_A = f_A\,(x_A, x_B, x_C) = B_{AB}\,x_B^2 + B_{AC}\,x_C^2 + (B_{AB} + B_{AC} - B_{BC})\,x_B\,x_C \quad (1)$$

The binodal (mutual-solubility) curve is then obtained by iterative simultaneous solution of three activity equations of the following type, one for each component:

$$(\ln a_A =)\ \ln x_{A1} + f_A\,(x_A, x_B, x_C)_1 = \ln x_{A2} + f_A\,(x_A, x_B, x_C)_2 \quad (2)$$

The spinodal curve, which separates the metastable from the unstable region (*19, 24*), is given by

* No intersections that are not matched three-way intersections will lie on the path formed by the matched three-way intersections; this leads to the conclusion that points representing only partial equilibrium (that is, equal activities of one, or two, components) must lie off the solubility curve. Further, a single-phase ternary mixture has no thermodynamic preference for, or knowledge of, a solubility-curve composition; from this one concludes that a single phase can be in the metastable region without preferring to be elsewhere.

$$B_{AB}\,x_A\,x_B + B_{AC}\,x_A\,x_C + B_{BC}\,x_B\,x_C + \frac{1}{2}\,(L\,x_A\,x_B\,x_C - 1) = 0 \quad (3)$$

with $L = (B_{AB} - B_{AC} - B_{BC})^2 - 4B_{AC} \cdot B_{BC}$. This curve becomes tangent to the mutual-solubility curve at one point only, the critical or plait point.

Application to a Typical Case

The idealized ternary system to be used is modeled after the system *n*-decane (*A*)/butadiene (*B*)/furfural (*C*), for which experimental data have been reported by Smith and Braun (*27*). The binary constants selected are $B_{AC} = 0.7396$, $B_{BC} = 1.5376$, and $B_{AB} = 4.4100$. Because the square roots of these constants are additive (that is $B_{AB}^{1/2} = B_{AC}^{1/2} + B_{BC}^{1/2}$) L is equal to zero, and curves of constant activity coefficient for the three components are all linear and parallel to the set for *A* shown in Figure 1. This type of addivity conforms to the Hildebrand solubility-parameter treatment of nonideal solutions (*16*).

A two-phase ternary system is characterized by six concentrations. Of these, one (for instance x_{C1}) may be taken as the independent variable. Two others (x_{A1} and x_{B2}) are eliminated by material balance. The remaining three are determined by solving three simultaneous equations, each having the form of Equation (2). This set is most easily solved by repeated iteration which lends itself to use of a digital computer. First a trial set of concentration values is assumed and is used to evaluate the activity-coefficient terms (fs). The equation for a_C is then solved for x_{C2}, and the remaining equations are solved simultaneously for x_{B1} and x_{A2}. The results are used as a new trial set, and iteration is repeated until the results converge.

The equilibrium curve constructed in this manner is shown in Figure 2; tie-line behavior is indicated by the usual type of conjugate line. For reference the spinodal curve obtained from Equation (3) is also shown. (The remaining curves of this figure will be described later.)

In order to interrelate activity and composition on the left-hand branch of the equilibrium curve, the numerical results for the latter were fitted to polynomial equations by linear regression. The equations used are

$$x_{C1} = \alpha_{(1)}\,a_{C1} + \alpha_{(2)}\,a_{C1}^2 + \alpha_{(3)}\,a_{C1}^3 + \alpha_{(4)}\,a_{C1}^4 \quad (4)$$

and

$$x_{B1} = \beta_{(1)} + \beta_{(2)}\,x_{C1} + \beta_{(3)}\,x_{C1}^2 + \beta_{(4)}\,x_{C1}^3 + \beta_{(5)}\,x_{C1}^4 + \beta_{(6)}\,x_{C1}^5 \quad (5)$$

In order, the α values are 0.49556, 0.49156, −0.13455, and 1.6134; the β's are 0.013508, 0.049664, 0.034766, 0.53246, −1.3367, and 2.0677. When a value of a_{C1} is used for solving equations and the resulting compositions are then used in Equations (1) or (2), the mean deviation between the input and output a_{C1} is 3×10^{-5} activity unit.

SCOPE OF THE MASS TRANSFER CALCULATIONS

Comparative calculations are reported in this paper for a number of countercurrent extraction runs utilizing the ternary system just described. Most of these calculated runs involve identical feed and solvent concentrations, identical extents of extraction of the distributed component (*C*), and nearly identical flow rates. The mass transfer ratios (k_{C2}/k_{C1}), (k_{B1}/k_{C1}), and (k_{A2}/k_{C1}) are all held constant in any one run and are varied separately in different runs to investigate their influence on the path of the extraction process.

The mass transfer resistance in each phase is assumed to lie between the bulk of the phase and the portion closest to the interface; equilibrium is assumed to exist at the interface, with the activity of each of the three components at that point having the same value in both phases. The driving potential that was assumed for the calculations is discussed in the next section.

The concentration paths followed by the two phases during each run have been calculated by a repetitive step-by-step procedure, starting at either the feed end or the solvent end of the column. Assumed values of exit composition were varied with respect to carrier components *A* and *B*, until the paths computed from the two directions agreed closely.

The equations used for these numerical calculations will be derived below, after a discussion of the mass transfer relations on which the calculations were based.

DRIVING POTENTIAL FOR MASS TRANSFER

The driving potential for transfer between phases is usually defined in terms of the concentration gradient in the vicinity of the interface, based upon broad experience with situations where activity coefficients within a phase are essentially constant. In these terms the rate of mass transfer is

$$N_B = k_{Bp}'\,(c_{Bp} - c_{Bpi}) + V^*c_{Bp} \quad (6)$$

In this treatment concentrations will be replaced by mole fractions, with k_{Bp} applying to such units. For nonideal solutions (with varying activity coefficients) the authors believe that concentration difference should be replaced by a modified activity difference that indicates more accurately the direction and relative magnitude of material transfer. Such an activity difference has been justified theoretically for molecular diffusion by Hartley (*13, 14*), Darken (*6*), Stearn and Eyring (*28*), Jost (*17*), and others.

Diffusion, as a molecular phenomenon, must depend upon the concentrations of molecules physically present. It is important to observe that the activity difference can be expressed in units of concentration, if it is divided by an appropriate mean activity coefficient. This quotient can therefore be considered as a modified concentration gradient, which evidently reduces to the familiar concentration-difference form when the activity coefficient is constant along the mass transfer path. Essentially the gradient of activity coefficient existing in nonideal solutions makes it easier for molecules to diffuse

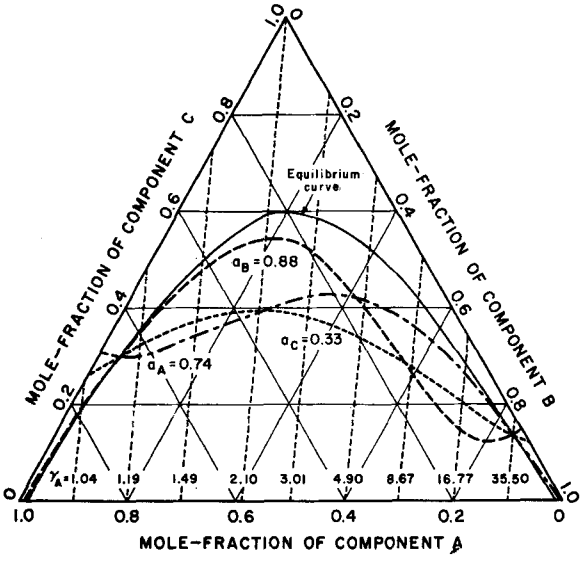

Fig. 1. Representative lines of constant activity coefficient (γ_A) and constant activity (a_A, a_B, a_C).

in one direction than in the other. These qualitative considerations may be replaced by the formal derivations to follow.

Diffusion is not the entire answer because turbulent transport often predominates and its mechanism is still very poorly understood. The writers believe that penetration theories provide the most detailed and most likely model of turbulent transport yet developed; these involve a steepening of the gradient that leads to molecular diffusion rather than its replacement by some other mode of transport. Handlos and Baron (*11*) report transport experiments where the rate is much higher than would result from quiescent molecular diffusion, but where the results still fit activity-gradient driving potentials rather than concentration gradient. Much additional experimental study is needed of nonideal solutions; meanwhile the problem remains in a state where concentration-difference driving potentials, although used traditionally, have never been proved to apply and are probably incorrect.

It is not essential to use the activity-gradient driving potential in order to solve the present problem, and the results obtained are not influenced critically by this particular choice of a potential. Rather this choice has been made in the belief that it is fundamentally the most accurate one available.

Diffusion in Nonideal Solutions

The basic reactions will be derived for binary systems, and the ternary systems of interest will then be treated (with due attention to thermodynamic requirements) as extensions of a binary system.

For a binary system *A-B* the mass rate of transfer of a component *A* relative to the mass average velocity, uncorrected for bulk flow, at constant temperature, has been given by Bird, Stewart, and Lightfoot (2) as

$$j_A = \frac{C_t^2}{\rho RT} M_A M_B D_{AB} x_B \frac{dG_B}{dx_A} \cdot \frac{dx_A}{db} \qquad (7)$$

Equation (7) can be transformed to a relation for the molar flux J_A^* under equimolal counterdiffusion (that is relative to a zero molar-average velocity) by means of the methods of Bird et al. (2):

$$J_A^* = \frac{C_t}{RT} D_{AB} x_B \frac{d\bar{G}_B}{db} \qquad (8)$$

Similarly for component *B*

$$J_B^* = \frac{C_t}{RT} D_{AB} x_A \frac{d\bar{G}_A}{db} \qquad (9)$$

Since the molar-average velocity is zero, $J_A^* = -J_B^*$. Equations (8) and (9) thus conform to the Gibbs-Duhem equation, $x_B\, d\bar{G}_B = -x_A\, d\bar{G}_A$.

Activity units will now be introduced. By reference to the component of interest in its pure liquid state

$$\bar{G}_B = \bar{G}_{BO} + RT \ln a_B = \bar{G}_{BO} + RT \ln (\gamma_B x_B) \qquad (10)$$

Substitution in Equation (8) gives

$$J_B^* = -J_A^* = -\frac{C_t D_{AB}}{\gamma_B} \frac{d a_B}{db} \qquad (11)^*$$

If material transfer is examined in a single region of an extraction tower, at steady state, the molar flux J_B^* will be a constant at all points in the vicinity of the interface, in the direction of transfer. Hence Equation (11) can be integrated between the interface and the bulk phase, by separating the variables:

$$J_B^* \int_0^b db = -\int_{a_B}^{a_{Bi}} \frac{C_t D_{AB}}{\gamma_B} da_B \qquad (12)$$

For transfer within either phase C_t and D_{AB} will be nearly constant, and γ_B may be replaced by an approximate average value γ_{Bm}, also treated as constant. These assumptions provide the result:

$$J_B^* = \frac{C_t D_{AB}}{b} \cdot \frac{a_B - a_{Bi}}{\gamma_{Bm}} \qquad (13)$$

Clearly one wishes to select a mass transfer coefficient that will be as nearly constant as possible. If this coefficient is taken as $k_B = C_t D_{AB}/b$, then

$$J_B^* = \frac{k_B}{\gamma_{Bm}} (a_B - a_{Bi}) \qquad (14)$$

In any practical case C_t, D_{AB}, and b will each vary somewhat over a range of conditions, and hence k_B will not actually be constant. However the precise pattern of variation of k will depend upon the particular system involved. For a system where molar densities, D_{AB}, and viscosity are known as functions of composition, k's determined from them can be used in the step-by-step calculations to be described. Instead in the general and abstract problem considered here the effect of possible variations in k can be treated most explicitly by solving the problem repeatedly for different constant values of k. Since changing k produces a relatively uniform trend in column behavior, the result for a range of variation in k in any practical solution must lie between the types of behavior calculated for the highest and lowest k values in the range.

By using Equation (14) in an overall relation for net transport, one arrives at the following extension of Equation (6) which appears to provide the most nearly correct simple form for nonideal binary solutions:

$$N_B = \frac{k_{Bp}}{\gamma_{Bpm}} (a_{Bp} - a_{Bi}) + N_t x_{Bpm} \qquad (15)$$

Penetration Theory

The penetration theory relates turbulent transport to molecular diffusion in certain cases (*15*, 5). By a procedure analogous to the usual development (in terms of concentration driving potential) of Fick's second law from his first law, Equation (11) can be shown to yield

$$\frac{\partial x}{\partial t} = \frac{D_{AB}}{\gamma} \frac{\partial^2 a}{\partial b^2} \qquad (16)$$

By introducing only the relation between activity and concentration, one finds that

$$\frac{\partial x}{\partial t} = \frac{\partial a}{\partial t} \cdot \frac{1}{\gamma \left(\frac{\partial \ln a}{\partial \ln x} \right)} \qquad (17)$$

From Equations (16) and (17)

$$\frac{\partial a}{\partial t} = D_a \frac{\partial^2 a}{\partial b^2} \qquad (18)$$

where

$$D_a = \left(\frac{\partial \ln a}{\partial \ln x} \right) D_{AB} \qquad (19)$$

With the introduction of a_j and a_i as the bulk and interface activity values, with an infinite concentration gradient at zero time, and with the assumption that local values of $(\partial \ln a/\partial \ln x)$ can be replaced by an average value across the transport path, the solution of Equation (18) becomes

$$\frac{a - a_j}{a_i - a_j} = \text{erf}\left(\frac{b}{2\sqrt{D_a t}} \right) \qquad (20)$$

where erf represents the error function, defined by the relation

$$\text{erf } V = \frac{2}{\sqrt{\pi}} \int_0^V e^{-z^2} dz \qquad (21)$$

* An alternate approach used by some investigators, among them De Groot (9), Denbigh (7), Miller (22), and Harned and French (12) involves a thermodynamic-potential gradient:

$$J_B^* = -\mathcal{D} \frac{d\mu_B}{db} = -\frac{1}{\gamma_B} \left(\frac{\mathcal{D} RT}{x_B} \right) \frac{da_B}{db} \qquad (11a)$$

The coefficient $\mathcal{D}RT/x_B$ thus replaces $C_t D_{AB}$. There are two reasons for believing that D_{AB} (or $\mathcal{D}/x$) is more constant than $\mathcal{D}$. The first is that, for ideal solutions, $J^* \propto \mathcal{D}\,(d \ln x_B/db)$ rather than $D_{AB}(dx_B/db)$; for such solutions all available experimental data favor the constancy of D_{AB}. The second reason is the molecular nature of diffusion; changes in thermodynamic potential result from changes in molecular composition, rather than the reverse.

A third possibility for a thermodynamic formulation of the driving potential would utilize the fugacity (or activity), as indicated by Opfell and Sage (23), Johnson (18), and Birchenall and Mehl (1). This alternative also reduces to the simple concentration-gradient form for ideal solutions but appears not to have the same theoretical support as Equation (11). (Compare reference 17). Tests of the modified activity driving potential must allow for any change in viscosity or permeability of the medium and also must treat activity coefficient as a point function, since only the nature of its variation along the diffusion path is expected to influence the diffusion rate. Thus a recent discussion of polyethylene diffusivities by Henley and Prausnitz, *A.I.Ch.E. Journal*, 8, 133 (1962), did not include a test of the present Equation (11).

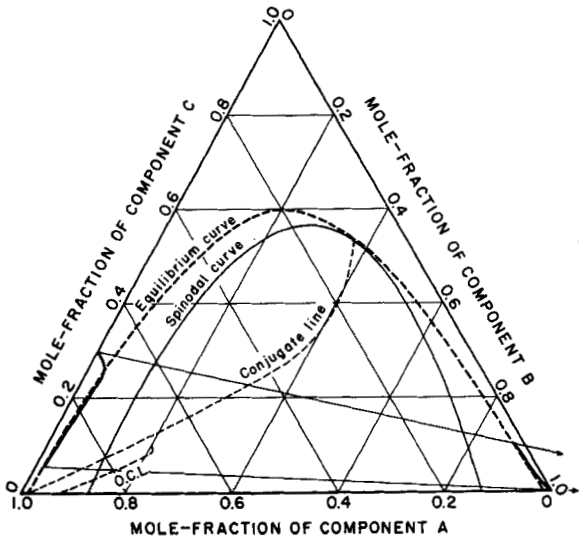

Fig. 2. Equilibrium diagram for idealized ternary system. Calculated concentration profiles shown for $k_{C2}/k_{C1} = 1$, $k_{B1}/k_{C1} = 1$, $k_{A2}/k_{C1} = 1$ with points related by the operating conjugate line (O. C. L.).

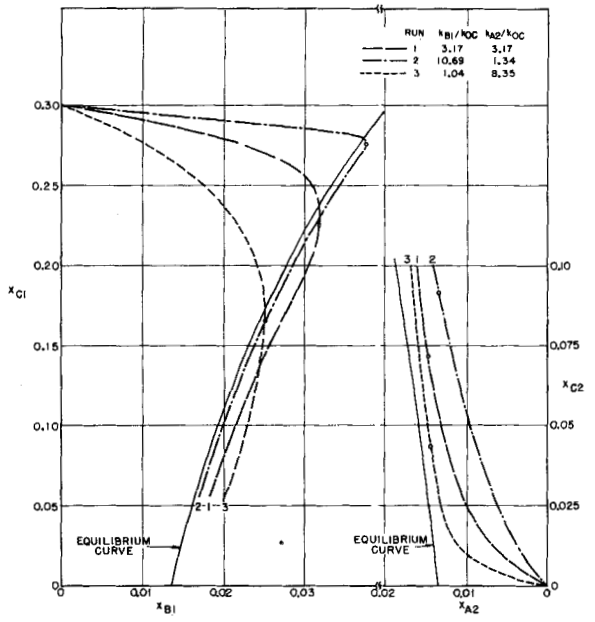

Fig. 3. Calculated concentration profiles showing the effect of the k_{B1}/k_{CC} ratio.

The amount of material diffusing through the interface is equal to

$$J^* = -\frac{C_t D_{AB}}{\gamma}\left(\frac{\partial a}{\partial b}\right)_{b=0} \quad (22)$$

or, from differentiation of Equation (20)

$$J^* = -\sqrt{\frac{D_{AB}}{\pi t}}\frac{C_t(a_i - a_j)}{\gamma_i\left(\frac{\partial \ln a}{\partial \ln x}\right)_m^{1/2}} \quad (23)$$

By defining a new diffusion coefficient

$$D' = \frac{D_{AB}}{\left(\frac{\partial \ln a}{\partial \ln x}\right)_m} \quad (24)$$

Equation (20 may be rewritten as

$$J^* = \sqrt{\frac{D'}{\pi t}}\frac{C_t(a_j - a_i)}{\gamma_i} \quad (25)$$

This result has the important significance that, in the particular case corresponding to the penetration-theory model, the direction of the activity gradient is shown to govern the direction of turbulent diffusion as well as that of molecular diffusion. By assuming as before that $\gamma_i = \gamma_m$, one observes in Equation (25) that the effective mean activity coefficient is an essential factor in relating the activity driving-potential to the rate of mass transfer.

Comparison of Equations (14) and (25) shows that the correction factor introduced in Equation (24) would enter the mass transfer coefficient as a square root. Calculations on the idealized ternary system indicate that the square root varies appreciably from a constant value, but its variation usually lies within a factor of $\sqrt{2}$. Since this range of variation would not affect the qualitative conclusions to be drawn, the molecular-diffusion relation of Equation (14) has been used instead of the penetration-theory result of Equation (25) as the basis of calculations.

Ternary-System Behavior

Each of the two phases under consideration may be viewed as containing two (or one) major components, with the remaining one (or two) always under 6 mole %, and usually under 3 mole %, of the total phase. As an approximation which again serves an exploratory purpose the transport of the major solute will be calculated from its binary behavior with the solvent; the transport of the minor component will be calculated from binary diffusion, regarding the mixture of the two major components as if it were a single compound; and transport of the solvent will then be obtained by difference.

This procedure will be outlined algebraically for phase 1, where A is the major component, B the minor one, and C the solute. For the solute Equation (15) converts to the form

$$N_C = \frac{k_{C1}}{\gamma_{C1m}}(a_{C1} - a_{Ci}) + N_t x_{C1m} \quad (26)$$

For the minor component also

$$N_B = \frac{k_{B1}}{\gamma_{B1m}}(a_{B1} - a_{Bi}) + N_t x_{B1m} \quad (27)$$

where

$$N_t = N_A + N_B + N_C \quad (28)$$

Theoretically each phase possesses three independent mass transfer coefficients modeled after three independent diffusion coefficients. This number is obtained, for instance, from irreversible-thermodynamic considerations [De Groot (9)]; Bird (2) also indicates this number to be necessary, since each binary pair necessarily introduces its respective value. The behavior of the minor component averages the effects of two of the binary coefficients (2, 30):

$$D_{B,mix} = \frac{x_A + x_C}{\frac{x_A}{D_{BA}} + \frac{x_C}{D_{BC}}} \quad (29)$$

By a material balance with Equation (28) the equation for diffusion of solvent is

$$N_A = -\frac{k_{C1}}{\gamma_{C1m}}(a_{C1} - a_{Ci}) - \frac{k_{B1}}{\gamma_{B1m}}(a_{B1} - a_{Bi}) + N_t(x_{A1})_m \quad (30)$$

but N_A can also be calculated from the relation

$$N_A = \frac{k_{A1}}{\gamma_{A1m}}(a_{A1} - a_{Ai}) + N_t(x_{A1})_m \quad (31)$$

If k_{C1} and k_{B1} are constants, k_{A1} is not a constant but must be calculated as follows. The equimolal-counterdiffusion terms must add to zero:

$$\frac{k_{C1}}{\gamma_{C1m}}(a_{C1} - a_{Ci}) + \frac{k_{B1}}{\gamma_{B1m}}(a_{B1} - a_{Bi}) + \frac{k_{A1}}{\gamma_{A1m}}(a_{A1} - a_{Ai}) = 0 \quad (32)$$

The Gibbs-Duhem relation can take the form

$$\frac{da_A}{\gamma_A} + \frac{da_B}{\gamma_B} + \frac{da_C}{\gamma_C} = 0 \quad (33)$$

Integration between the interface and the bulk phase, with the assumption of constant γ's, gives

$$\frac{a_{A1} - a_{Ai}}{\gamma_{A1m}} + \frac{a_{B1} - a_{Bi}}{\gamma_{B1m}} + \frac{a_{C1} - a_{Ci}}{\gamma_{C1m}} = 0 \quad (34)$$

From this the following expression is obtained:

$$k_{A1} = \frac{\dfrac{k_{C1}(a_{C1}-a_{Ci})}{\gamma_{C1m}} + \dfrac{k_{B1}(a_{B1}-a_{Bi})}{\gamma_{B1m}}}{\dfrac{a_{C1}-a_{Ci}}{\gamma_{C1m}} + \dfrac{a_{B1}-a_{Bi}}{\gamma_{B1m}}} \quad (35)$$

The calculations to follow will thus be based upon four adjustable mass transfer coefficients: k_{C1} and k_{B1}, for phase 1 in which component A predominates; and k_{C2} and k_{A2}, for phase 2 in which component B predominates. Moreover, as one is concerned with relative values of these coefficients, k_{C1} will be used as reference. The ratios k_{B1}/k_{C1}, k_{C2}/k_{C1}, and k_{A2}/k_{C1} will then need to be defined for each calculated *run*, or steady state condition of column operation.

CALCULATION PROCEDURE

Material Balance

For an incremental section of an extraction column with unit cross-sectional area normal to the directions of flow, the mass transfer of component C between immiscible phases in countercurrent flow can be expressed by

$$\Delta n_C = \Delta(F_1 x_{C1}) = \Delta(F_2 x_{C2}) \quad (36)$$

and similarly for each other component. A total rate of transfer for each component (for example n_C) is now defined by the relation

$$n_C = A\,h\,N_C \quad (37)$$

For an incremental height

$$\Delta n_C = A\,N_C\,\Delta h \quad (38)$$

Mass Transfer

Equation (26) takes the form, for phase 1

$$\Delta n_C = (\Delta n_t)\,x_{C1m} + \frac{k_{C1}\,A\,\Delta h}{\gamma_{C1m}}(a_{C1}-a_{Ci}) \quad (39)$$

where $\Delta n_t = A\,N_t\,\Delta h$. The approximation is now introduced that x_{Ci} can replace x_{C1m} and γ_{Ci} can replace γ_{C1m}. This simplifies the calculations that are to be made by eliminating an iterative calculation of the true mean values; the error thus introduced in the local rate of mass transfer is always under 10% and usually under 5%, and it has a still smaller effect on the comparison of calculations with different k values. Therefore as a basis for step-by-step calculations the following relation is adopted:

$$\Delta n_c = \Delta(F_1 k_{C1}) \quad (40a)$$

$$= (\Delta n_t)\,k_{C1} + \frac{k_{C1}\,A\,\Delta h}{\gamma_{C1}}(a_{C1}-a_{Ci}) \quad (40b)$$

with similar relations for the remaining components in phase 1 and all components in phase 2.

Calculation of Any One Column Increment

An arbitrary, convenient, and uniform small increment Δx_{C1} (which is negative for calculations starting at the feed end and positive for those starting at the solvent end) is now selected. Through Equation (40a) this fixes the value of Δn_C to be used in the first step. The driving potentials that apply at the start of each increment are assumed to remain constant throughout the increment. The size of Δx_C is reduced in successive runs by factors of one half to a value (usually 0.002) where the column profiles have become independent of the increment used.

As Δn_t is not known, it must be determined by iteration, starting with $\Delta n_t \approx \Delta n_C$ as the first trial value. If this assumption is used, Equation (40b) yields the relation

$$\Delta n_c = \frac{k_{C1}\,A\,\Delta h(a_{C1}-a_{Ci})}{\gamma_{C1}(1-x_{C1})} \quad (41a)$$

$$= \frac{k_{C2}\,A\,\Delta h(a_{Ci}-a_{C2})}{\gamma_{C2}(1-x_{C2})} \quad (41b)$$

As knowledge of interface conditions is needed to use the individual-phase mass transfer coefficients, Equations (41a) and (41b) can be solved for the interface activity a_{Ci}, with the result

$$a_{Ci} = \frac{a_{C1}\dfrac{k_{C1}}{k_{C2}}\cdot\dfrac{1-x_{C2}}{1-x_{C1}} + \dfrac{\gamma_{C1}}{\gamma_{C2}}a_{C2}}{\dfrac{\gamma_{C1}}{\gamma_{C2}} + \dfrac{k_{C1}}{k_{C2}}\cdot\dfrac{1-x_{C2}}{1-x_{C1}}} \quad (42)$$

Main Calculational Sequence

Use of Equations (4) to (5) defines the interface concentration in phase 1, and Equation (1) then defines the remaining interface activities a_{Ai} and a_{Bi}. These are the same for both phases, under the authors' assumption of equilibrium at the interface. The relative height of column required for the selected increment of transfer is then given by the expression

$$k_{C1}\,A\,\Delta h = \frac{(\Delta n_C)(1-x_{C1})}{x_{C1}-\dfrac{a_{Ci}}{\gamma_{C1}}} \quad (43)$$

with a_{Ci} obtained from Equation (42). From this point on, $k_{C1}\,A\,\Delta h$ is used as a fixed value, and Δk_{C1} and Δn_C are allowed to vary from the input values.

By means of relations of the form of Equation (40b), applied to phase 1 for component B and to phase 2 for component A, with substitutions of the type

$$k_{B1}\,A\,\Delta h = (k_{B1}/k_{C1})\,k_{C1}\,A\,\Delta h \quad (44)$$

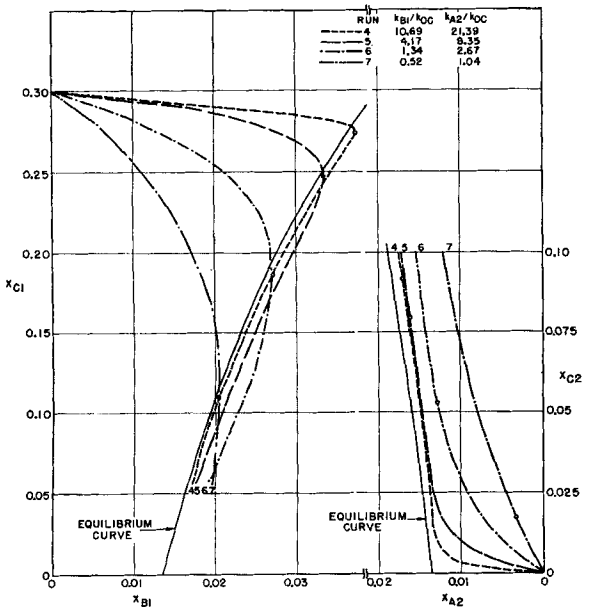

Fig. 4. Calculated concentration profiles showing the effect of the k_{B1}/k_{OC} and k_{A2}/k_{OC} ratios.

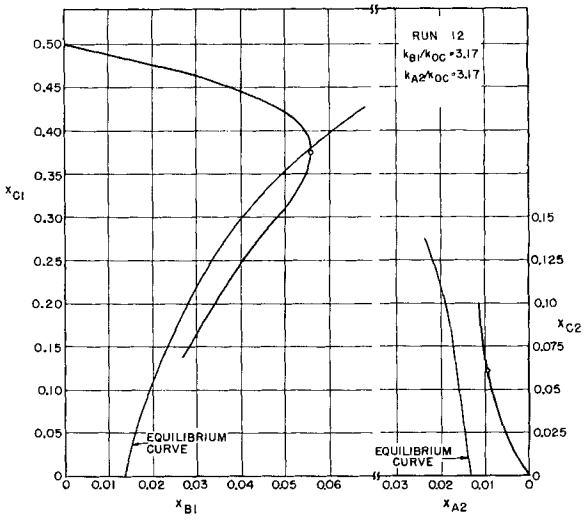

Fig. 5. Calculated concentration profile for a feed with higher concentration of C.

TABLE 1. EFFECT OF MASS TRANSFER COEFFICIENT RATIOS ON EXIT CONCENTRATIONS

Run no.	k_{C2}/k_{C1}	k_{B1}/k_{C1}	k_{A2}/k_{C1}	k_{B1}/k_{OC}	$(x_{B1})_{out}$	k_{A2}/k_{OC}	$(x_{A2})_{out}$
9	0.5	4.0	2.0	21.39	0.01698	10.69	0.01724
2	0.5	2.0	0.25	10.69	0.01699	1.34	0.01420
4	0.5	2.0	4.0	10.69	0.01685	21.39	0.01718
11	2.0	4.0	2.0	8.35	0.01738	4.17	0.01700
5	2.0	2.0	4.0	4.17	0.01756	8.35	0.01817
1	1.0	1.0	1.0	3.17	0.01778	3.17	0.01627
8	0.5	0.5	0.25	2.67	0.01783	1.34	0.01389
6	0.5	0.25	0.5	1.35	0.01927	2.67	0.01580
3	2.0	0.5	4.0	1.04	0.02000	8.35	0.01699
10	2.0	0.5	0.25	1.04	0.02011	0.52	0.00875
7	2.0	0.25	0.5	0.52	0.0210	1.04	0.01170

Δn_A and Δn_B (and Δn_C) are determined. A revised Δn_t is then found as the sum of $(\Delta n_A + \Delta n_B + \Delta n_C)$.

Preparation for Next Step of Iteration

This new value of Δn_t may be taken as the starting point for the next round. This second round of calculation requires a new determination of the interface conditions, since Equation (42) is no longer applicable. The value of a_{Ci} can again be eliminated between the rate terms for component C in phases 1 and 2, as obtained from relations of the type of Equation (40b):

$$a_{Ci} = \frac{\dfrac{\Delta n_t (x_{C1} - x_{C2})}{k_{C1} A \Delta h} + x_{C1} + \dfrac{k_{C2}}{k_{C1}} x_{C2}}{\dfrac{1}{\gamma_{C1}} + \dfrac{1}{\gamma_{C2}} \dfrac{k_{C2}}{k_{C1}}} \qquad (45)$$

This value of a_{Ci} allows one to re-enter the main calculational sequence. In the present calculations both a second and a third round were made in this way.

Completion of Incremental Calculation

When the input and output values of Δn_t have converged adequately (to within $\pm 1.0\%$), the values of Δn obtained can be used to determine the overall changes in concentration. Equations of the following type (illustrated for component C) will be used for each component in each phase over the increment:

$$(F_1)_{end} = (F_1)_{start} + \Delta n_t \qquad (46)$$

$$(n_{C1})_{end} = (n_{C1})_{start} + \Delta n_{C1} \qquad (47)$$

$$(x_{C1})_{end} = (n_{C1})_{end}/(F_1)_{end} \qquad (48)$$

Similar equations apply to phase 2. These last equations complete the calculation for any one step.

Overall Calculation Scheme

Most of the runs calculated for comparison were based upon nearly the same flow rates and extents of extraction and involved transfer of the distributed component (C) from phase 1 into phase 2. The conditions specified, at the top of the column, were

$(F_1)_{in} = 1.000$ $\qquad$ $(F_2)_{out} = 2.600$
$(x_{C1})_{in} = 0.30$ $\qquad$ $(x_{C2})_{out} = 0.10$
$(x_{B1})_{in} = 0.0$

and at the bottom of the column

$(x_{C2})_{in} = 0.0$
$(x_{A2})_{in} = 0.0$

The averages of the material-balance results determined by the step-by-step solutions were

$(F_1)_{out} = 0.72$ $\qquad$ $(F_2)_{in} = 2.32$
$(x_{C1})_{out} = 0.056$

The major differences resulting from a change in the k ratios were in the values of $(x_{B1})_{out}$ and $(x_{A2})_{out}$. Calculations were normally started at the top of the column, with an assumed value of $(x_{A2})_{out}$. Unless the correct value was used, to at least three significant figures, the calculation would not converge upon the specified bottom-end conditions. The way in which the profiles deviated from the expected behavior was used as a basis for altering the assumed value of $(x_{A2})_{out}$, and this was taken as the starting condition for the next trial calculation. The criteria for identifying unsatisfactory profiles were built into a computer program so that the successive trial values were arrived at automatically.

When satisfactory convergence was obtained in reaching the bottom-end conditions, the resulting values of $(x_{C1})_{out}$, $(F_1)_{out}$, and $(F_2)_{in}$ were taken as input for a calculation up the column. In almost every case these reversed calculations confirmed the previous result. In two cases convergence was not obtained when $(x_{A2})_{out}$ or $(x_{B1})_{out}$ was preset to the nearest digit in the eighth significant figure; in these cases the true curves could be determined readily by interpolation.

Results

The results of the step-by-step calculations are reported in Table 1 and Figures 2 through 6, which record the concentration path followed by each phase inside the column.

In Figure 2 the pair of concentration profiles calculated for $k_{C2}/k_{C1} = 1$, $k_{B1}/k_{C1} = 1$, $k_{A2}/k_{C1} = 1$ (a 1-1-1 run) is plotted on the triangular graph. Lines are projected through coexisting points of the concentration path to form an operating conjugate line (O.C.L.), as well as the usual operating point (off the plot, to the right).

However in Figure 2 the scale of the triangular plot conceals the difference between the actual profile and the equilibrium curve. Rectangular coordinates allow greater flexibility in choice of scales and provide a much clearer view of the concentration-profile behavior.

Figure 3 shows, as Run 1, the 1-1-1 run from Figure 2. Two other runs are shown, for which k_{B1}/k_{C1} and k_{A2}/k_{C1} vary in opposite directions. To give an idea of the coexisting points in each run the height in the column corresponding to the knee of the phase-1 curve is identified by a point on each of the two curves for the run. Figure 4 shows a series of runs, for which k_{B1}/k_{C1} and k_{A2}/k_{C1} are always on the same side of unity; again the knee points are identified.

In both figures the concentration path followed by the three components falls partly inside the equilibrium curve for phase 1 but stays outside for phase 2. This crossing over is quite general and occurs for whatever k ratios were chosen. However the rapidity with which each concentration profile approaches the respective equilibrium curve depends largely on the k ratios.

The concentration profiles for the two phases behave somewhat independently. In Figure 3 the run that lies farthest inside the two-phase region for phase 1 (Run 3) is nearest the equilibrium curve for phase 2, but in Figure 4 the run that is farthest on one side is also the farthest on the other (Run 7).

In addition to the runs shown in Figures 3 and 4 four calculations were made (Runs 8 through 11) with the same end conditions but with still other sets of mass transfer coefficients. Since the results are similar to and consistent with those shown in Figures 3 and 4, they are not plotted separately but are included in Table 1. The nearness with which equilibrium is approached, as a stream leaves the column, is indicated by the outlet $(x_A)_2$ and $(x_B)_1$ values; at equilibrium these would be respectively 0.01878 (precisely) and 0.0165 [approximately, owing to small variations in the outlet value of $(x_C)_1$].

Two other extraction runs with unit ratios of the mass transfer coefficients (hence 1-1-1 runs) were also calculated. Figure 5 shows the concentration path for a feed richer in $C(x_{C1} = 0.50)$, calculated with a correspondingly higher relative flow rate for phase 2. Again the crossing over occurs for phase 1 but not for phase 2. Figure 6 shows a reverse extraction at essentially the same feed-rate ratio used in most of the forward calculations. For interpreting the results of the calculations it

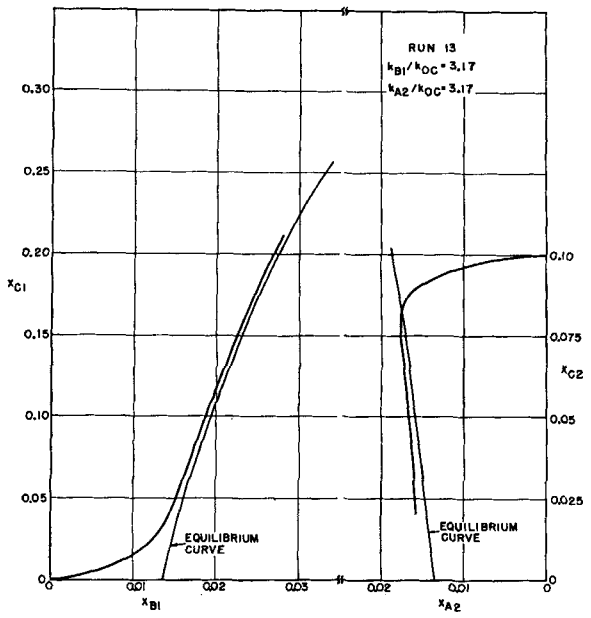

Fig. 6. Concentration profile for reverse extraction.

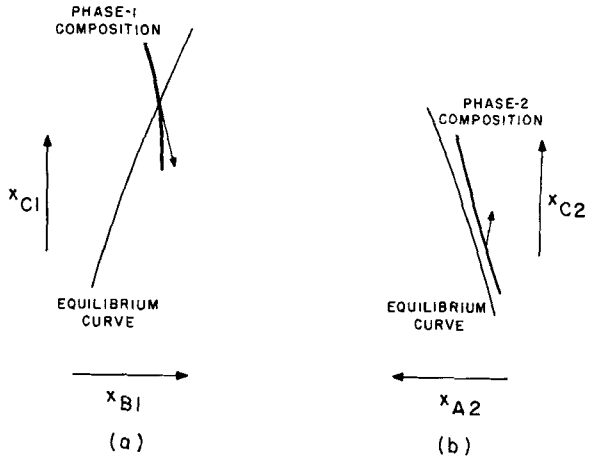

Fig. 7. Depletion and enrichment effects for compound C.

is significant that the concentration path for this reverse run crosses the equilibrium curve for phase 2 but not for phase 1

DISCUSSION

Crossing of the Equilibrium Curve

In order to explain this crossing of the equilibrium curve several factors must be considered. The crossing is not due solely to flow conditions because at constant relative flow rate the crossing depends on the direction of extraction. It is more correct to say that the effect is due to a nonequilibrium which is produced by the flow. Two principal factors must be considered: the effect of depletion (or enrichment) of component C, and the activity behavior of the minor component in each phase.

Depletion (or enrichment) of C. When the composition reaches the equilibrium line for phase 1 in the forward runs, the driving potential for B is close to zero and the rate of transfer of A is around one tenth that of C. As already indicated, each phase of the system is characterized by its respective activities which in themselves do not provide any abrupt indication that the composition has reached or crossed the equilibrium curve. Thus the behavior of the phase depends mainly upon the relatively large rate of depletion of C (in the forward case). Since the A/B ratio varies quite slowly, this depletion tends to pull the composition inside the curve (see Figure 7*a*).

For phase 2 in the forward case enrichment of C provides the major effect. In this phase this enrichment carries the concentration path away from the equilibrium line and thus keeps it from crossing (Figure 7*b*).

For the reverse case the opposite situation is encountered; the depletion effect of C in phase 2 carries the concentration path across the equilibrium curve, and the enrichment effect of C in phase 1 pulls it away from it.

Activity effects. From the slope of the constant-activity lines no transfer of B from phase 1 (or of A from phase 2 in the reverse case) will occur, except through bulk flow, until the composition is appreciably inside the equilibrium line. In the forward case the activity gradient for B in phase 1 changes in sign only after phase 1 has crossed the equilibrium curve. Physically this means that for a time after phase 1 enters the column it is enriched in B; then, after it is well inside the equilibrium curve, it rejects B again. This behavior is most easily explained by Figure 8, which shows the situation that prevails for phase 1 in the forward case.

Point I, in this figure, represents in a general way the equilibrium composition of the interface corresponding to some particular bulk-phase composition of phase 1. The line of constant activity for component B, through point I, lies inside the equilibrium curve in the region where x_c exceeds x_{c1} (that is where component C is being removed from phase 1). As the bulk composition moves diagonally to the right, the interface and its a_{Bi} line move downward. The intersection E' of the composition line with the a_{Bi} line shows the instantaneous situation where a_{B1} has overtaken a_{Bi} and the activity gradient is in process of changing sign. In this situation the system may be said to register the attainment of a partial equilibrium; however the point where it is reached is seen not to lie exactly on the static-equilibrium curve.

A similar explanation applies in the reverse case to component A in phase 2. Here also the concentration change due to the diffusion of A first acts in the same direction as that due to C; then, after the composition is appreciably inside the two-phase region, the diffusion of A begins to have an opposite effect.

Figure 1 shows that the slope of the constant-activity lines for B in phase 1 (and A in phase 2) is quite steep, and this means that the partial-equilibrium point actually will lie quite close to the equilibrium line. However the composition must be inside the partial equilibrium before back diffusion of B can begin to compensate for forward diffusion of C.

As a primary conclusion it is fair to say that the solute-depletion (or solute-enrichment) effect is the most important one and is the main cause of crossing or not into the metastable region. The behavior of this ternary system may be compared with that of a binary system undergoing crystallization. The temperature coordinate in binary behavior is analogous to the C-component coordinate in the ternary system. Abstraction of C, like lowering of temperature, carries the system from an undersaturated to a supersaturated condition, after which diffusion toward the equilibrium is counterbalanced by further C abstraction or temperature lowering. The equilibrium (for that particular phase) thereafter is always approached from the supersaturated side.

Since the approximations in the authors' calculation of driving potentials appear to be comparable in their effect to a change in the numerical value of one or another of the mass transfer coefficients, these approximations appear not to affect the overall conclusions reached. First, a crossing over will generally occur in a phase for which the solute-depletion slope is steeper than the constant-mole-ratio

slope (for the carrier and the minor component in the phase). Second, decrease in the mass transfer coefficient for the minor component in the phase involved will cause the concentration profile to deviate more widely from the equilibrium line.

From the shapes of the graphs it is noted first that k_{c1} and k_{c2} work together to produce a transfer of component C. With $k_{c2}/k_{c1} < 1$, the restoring potentials for components A and B become relatively larger, and static equilibrium is more nearly approached. Because the effects of k_{c1} and k_{c2} do combine, the influence of the coefficients k_{A2} and k_{B1} is better explained by referring them to an overall mass transfer coefficient k_{oc}, given by

$$\frac{1}{k_{oc}} = \frac{1}{k_{c1}} + \frac{1}{mk_{c2}} \qquad (49)$$

In this relation m is the distribution coefficient $(x_{c2}/x_{c1})_{eq}$, whose mean value calculated from the equilibrium curve is 0.460. With $k_{c1} = 1$, and when k_{c2} takes the values 2.0, 1.0, or 0.5, the overall mass transfer coefficient k_{oc} equals 0.479, 0.315, or 0.187, respectively.

For Run 2 in Figure 3 and Run 4 in Figure 4, both having a high ratio of k_{B1}/k_{oc}, the profile is close to equilibrium in phase 1. For phase 2 the ration k_{A2}/k_{oc} governs, since the values are different in Runs 2 and 4, and the curves are different. Similarly a comparison of Run 3 of Figure 3 with Run 5 of Figure 4 shows that a high ratio of k_{A2}/k_{oc} carries the profile close to equilibrium in phase 2. For phase 1 the ratio of k_{B1}/k_{oc} governs.

The effect of k_{A2}/k_{oc} may be explained as follows. For phase 2 diffusion of A from phase 1 to phase 2 has the effect of pulling the concentration profile toward the equilibrium curve (whereas diffusion of C in the same direction pulls the profile away from the equilibrium curve). While the effect of A is not large enough to balance completely the effect of C, it does serve to determine how closely the profile for phase 2 will approach the equilibrium curve. For phase 1 the effect of k_{B1}/k_{oc} on the concentration path is consistent with having the diffusion of B oppose the diffusion of C and pull the concentration path back toward the equilibrium curve, when the composition is appreciably inside the two-phase region (as was discussed in the preceding section).

Calculation of the Number of Transfer Units

Extraction-tower performance is usually characterized by quantities first introduced by Chilton and Colburn and named by them *number of transfer units* and *height of a transfer unit.*

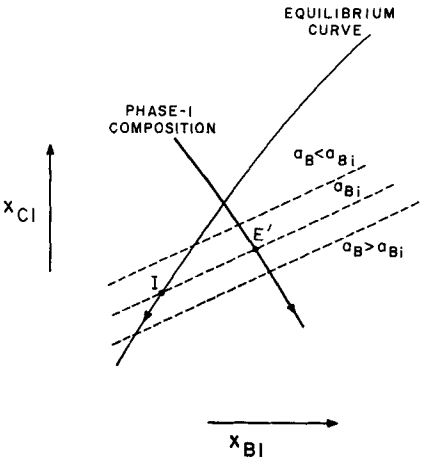

Fig. 8. Activity effect of the minor component on thermodynamic driving potential (phase 1).

These quantities can be defined for either phase 1 or phase 2, and on the basis of either a single-phase resistance or an effective overall resistance. They are related to column height in the following way:

Height of column = (function of mass transfer coefficients) × (function of separation performance) = (HTU) (NTU) (50)

Here HTU has dimensions of length, while NTU is dimensionless; within this restriction the definitions of the two must be compatible but are somewhat arbitrary. The usual practice is to define the NTU value for a component C with reference to a particular phase p, as

$$(\mathrm{NTU})_{cp} = \int_{(x_{Cp})_{in}}^{(x_{Cp})_{out}} \frac{d(\text{moles } C \text{ in phase } p)}{\text{relative driving potential for } C \text{ in } p} \qquad (51)$$

with the driving potential known as a function of the extent to which extraction has proceeded. Here, where the flow rate is not constant, the number of transfer units for component C in phase 1 can be defined as

$$(\mathrm{NTU})_{oc1} = \int_{(x_{C1})_{in}}^{(x_{C1})_{out}} \left\{ \left[1 - \frac{\Delta n_t}{\Delta n_c} x_{c1} \right] \frac{\gamma_{c1}}{(a_{c1} - a_{c2})(F_1)_{in}} \right\} d(F_1 x_{c1}) \qquad (52)$$

From the results of this investigation one may determine the effect of concentration profile upon NTU value. For the usual equilibrium-curve approximation to the profile the integrand term multiplying the differential in Equation (52) was plotted against $F_1 x_{c1}$ and was integrated numerically or graphically between the equilibrium-curve values in ($F_1 = 1.048$, $x_{c1} = 0.291$) and out ($F_1 = 0.732$, $x_{c1} = 0.056$)

The corresponding NTU values for the computed concentration profiles were evaluated as part of the computer calculation. The relation used was

$$\Delta(\mathrm{NTU})_{oc1} = \left[1 - \frac{\Delta n_t}{\Delta n_c} x_{c1} \right] \frac{k_{oc}}{k_{c1}} \cdot \frac{\gamma_{c1} \Delta n_{c1}}{(a_{c1} - a_{ci})(F_1)_{in}} \qquad (53)$$

where the γ, a, and F values were all evaluated at the start of each slice, and the increments were added cumulatively. The result of this calculation is identical to using $a_{c2} - a_{c1}$ as the driving potential and omitting the mass transfer coefficient ratio. The following values of overall NTU for component C relative to phase 1 were obtained:

Equilibrium-curve approximation	3.94
Run 1 (intermediate approach to equilibrium curve)	4.04
Run 7 (furthest departure from equilibrium curve in both phases	3.75
Run 5 (near approach to equilibrium curve in both phases)	4.00
Run 2 (near equilibrium curve in phase 1, far from equilibrium curve in phase 2)	4.74
Run 3 (near equilibrium curve in phase 2, far from equilibrium curve in phase 1)	3.75

If one compares Run 5 with the equilibrium-curve approximation, one sees that the NTU values are almost the same, because the concentration path for Run 5 is close to the equilibrium curve. For the other values, when the concentration path for phase 1 is far from equilibrium, the NTU value may either drop or rise, depending on whether the concentration path is mainly inside or mainly outside the equilibrium curve. On the other hand, when the concentration path for phase 2 is far from equilibrium, the NTU value rises. Thus one often deals with two opposite effects, and for intermediate cases one may get a partial compensation.

The effect just described can be explained with the help of the constant-activity line for component C, shown in Figure 1. With reference to a material-balance line drawn through an exterior operating point (which will be in nearly the same position for both the equilibrium-curve treatment and any concentration-profile calculation), it is seen that $a_{c1} < a_{c1E}$ when the concentration profile for phase 1 is inside the two-phase region. Thus the driving potential ($a_{c1} - a_{c2}$) is then smaller than the driving potential for the equilibrium-curve approximation, and the contribution of phase 1 to the NTU will be higher. When the concentration

profile for phase 1 lies outside the equilibrium curve, the driving potential is larger, and the NTU contribution will be less. In the same manner the constant-activity lines for component C show that when the concentration path for phase 2 is outside the two-phase region, a_{C2E} is less than a_{C2}. This leads to a smaller driving potential for $a_{C1} - a_{C2}$ and a higher NTU value than that of the equilibrium-curve approximation.

Run 2 shows the greatest rise in the NTU, resulting from increases due to both phase 1 and phase 2. Run 3 shows the greatest drop; here the drop from phase 1 outside the equilibrium curve overshadows the later rise due to phase 1 inside (and also the rise due to phase 2). Runs 1 and 7 reflect somewhat similar behavior.

CONCLUSIONS

The conditions and results of this investigation are as follows.

1. Activity differences as driving-potentials are more rigorous, from a thermodynamic standpoint, than the usual concentration driving-potential. In this work the activity difference has been selected on theoretical grounds and has been found convenient to use. The system taken for study is not so nonideal that an alternate choice of driving-potential would give a qualitatively different result.

2. The mass transfer coefficients selected are used as ratios to the value for the distributed solute in the raffinate phase. They are corrected for net bulk movement across the interface but otherwise are treated as constants. In each phase one coefficient is unspecified and is derived from the others by the Gibbs-Duhem relation. For any actual system the true extent of variation in mass transfer coefficient values should lead to profiles that would be bounded by the curves for different combinations of constant coefficients used in comparable theoretical calculations.

3. The concentration path does not approach the equilibrium curve instantaneously and then follow it, as is often assumed. Instead it may actually cross the equilibrium curve for one phase but stay away from it for the other.

4. The direction of diffusion of the transferring component (C in this study) is the main factor that determines whether a phase will cross the equilibrium line. For the usual case where the equilibrium shows an increase of the minor component in each phase as the transferring component is augmented, the phase that loses the transferring component is the one whose composition tends to cross the equilibrium curve.

5. The distance between the calculated concentration paths and the equilibrium line depends on the mass transfer coefficients. The larger the overall coefficient for component A, the nearer the phase 2 curve is to the equilibrium curve; the larger the overall coefficient for component B, the nearer phase 1 approaches the equilibrium curve.

6. Variation in the NTU values depends largely on the separation between the calculated concentration path and the equilibrium curve, in each phase. For extreme cases the number of transfer units calculated from the exact concentration path can differ as much as 10 to 20% from that calculated by the usual standard method.

7. Experimental verification of the calculated effects is needed. If the predicted effect is real, two-component analysis should replace single-component analysis of interior or terminal samples from operating extraction equipment involving ternary systems.

ACKNOWLEDGMENT

The authors express their thanks to the Lawrence Radiation Laboratory and the United States Atomic Energy Commission for financial support to Alphonse Hennico, and to the Miller Institute of Basic Research in Science at this University for support to Theodore Vermeulen during the course of this research. They are grateful to Professors Raymond Defay (University of Brussels), J. H. Hildebrand, J. M. Prausnitz, D. R. Olander, and F. A. Dullien (Oklahoma State University) for basic discussions of theoretical background and/or suggestions in regard to presentation of the results.

NOTATION

A = interfacial area per unit volume, sq. cm./cc.
a = activity
B = Margules constant, for Equation (1)
b = length coordinate, cm.
c,C = concentration, g.-moles/liter; C_t is total concentration or molar density
D = binary diffusion coefficient, sq. cm./sec.
D_a = modified diffusion coefficient [Equation (19)]
D' = modified diffusion coefficient [Equation (24)]
$\mathcal{D}$ = diffusion coefficient multiplying μ gradient [Equation (11a)]
d = differential operator
F = flowrate of a phase, g.-moles/sec./sq. cm.
f = function of
$\overline{G}$ = partial molal free energy, cal./g.-mole
HTU = height of a transfer unit, cm.
h = height in the extraction column, cm.
j = mass rate of transport, relative to mass-average velocity, g./sec./sq. cm.
J^* = molar rate of transport, relative to molal-average velocity, g.-moles/sec./sq. cm.
k,k' = mass transfer coefficient, (g.-mole/sec. sq. cm.)
(kA) = product of mass transfer coefficient and interfacial area per unit volume (g.-mole/sec. cc.)
L = function of Margules constants for a ternary system [Equation (3)]
M = molecular weight
m = distribution coefficient, $(x_{C2}/x_{C1})_{equil}$
N = rate of transfer, g.-moles per unit interfacial area per unit time
NTU = number of transfer units
n = rate of transfer, g.-moles per unit cross-sectional area per unit time
R = universal gas constant, cal. g.-mole °K.
T = absolute temperature, °K.
t = time
V = variable
V^* = molar-average velocity, cm. sec.
x = mole fraction
z = variable

Greek Letters

α = numerical constant [Equation (4)]
β = numerical constant [Equation (5)]
γ = activity coefficient, a/x
Δ = increment
ρ = density, g./cc.
μ = chemical potential, cal./g.-mole

Subscripts

A,B,C = components of the ternary system
E = equilibrium-line value
i = interface
j = bulk-phase
m = mean value
O = overall
p = phase
t = total
1 = phase rich in A
2 = phase rich in B

Superscript

* = equilibrium

LITERATURE CITED

1. Birchenall, C. E., and R. F. Mehl, *Metals Technol.*, **14**, T.P. 2168 (1947).
2. Bird, R. B., W. E. Stewart, and E. N. Lightfoot, "Transport Phenomena," pp. 497 to 502, 567 to 571, Wiley, New York (1950).
3. Chilton, T. H., and A. P. Colburn, *Ind. Eng. Chem.*, **27**, 255 (1935).

4. Colburn, A. P., and D. G. Welsh, *Trans. Am. Inst. Chem. Engrs.*, **38**, 143 (1942).
5. Danckwerts, P. V., *Ind. Eng. Chem.*, **43**, 1460 (1951).
6. Darken, L. A., *Metals Technol.*, **15**, T. P. 2311 (1948).
7. Denbigh, K. G., "Thermodynamics of the Steady State," Chap. 3 and 4, Methuen, London, England (1951).
8. Gibbs, J. Willard, "Collected Works," Vol. 1, pp. 105 to 115, Yale University Press, New Haven, Connecticut (1906).
9. de Groot, S. R., "Thermodynamics of Irreversible Processes," Chap. 7, North Holland Publishing Co., Amsterdam (1951).
10. Haase, Rolf, "Thermodynamik der Mischphasen mit einer Einführung in die Grundlagen der Thermodynamik," pp. 151 to 183, Springer Verlag, Berlin, Germany (1956).
11. Handlos, A. E., and Thomas Baron, *A.I.Ch.E. Journal*, 3, 127 (1957).
12. Harned, H. S., and D. N. French, *Ann. N. Y. Acad. Sci.*, 46, 267 (1945).
13. Hartley, G. S., *Phil. Mag.*, **12**, 473 (1931).
14. ———, and J. Crank, *Trans. Faraday Soc.*, **45**, 801 (1949).
15. Higbie, Ralph, *Trans. Am. Inst. Chem. Engrs.*, **31**, 365 (1935).
16. Hildebrand, J. H., and R. L. Scott, "The Solubility of Nonelectrolytes," Chap. 7, Reinhold, New York (1950).
17. Jost, Wilhelm, "Diffusion in Solids, Liquids, Gases," pp. 240 to 245, Academic Press, New York (1960).
18. Johnson, W. A., *Trans. Am. Inst. Min. Met. Engrs.*, **143**, 107 (1941).
19. Kortüm, Gustav, and Hertha Bucholz-Meisenheimer, "Die Theorie der Destillation und Extraktion von Flüssigkeiten, pp. 22 to 32, Springer Verlag, Berlin, Germany (1952).
20. Kuenen, J. P., "Theorie der Verdampfung und Verflüssigung von Gemischen und der Fraktionierten Destillation," pp. 68-69, Verlag, G. A. Barth, Leipzig (1906).
21. Laddha, G. S., and J. M. Smith, *Chem. Eng. Progr.*, 46, 195 (1950).
22. Miller, D. G., *Am. J. Phys.*, **24**, 433 (1956).
23. Opfell, J. B., and B. H. Sage, *Ind. Eng. Chem.*, **47**, 918, Equations (20) to (25) (1955).
24. Prigogine, Ilya, and Raymond Defay, "Chemical Thermodynamics," Chap. 16, Longmans-Green, New York (1954).
25. Reid, K. J., *J. Chem. Phys.*, 36, 55g (1962).
26. Sherwood, T. K., and R. L. Pigford, "Absorption and Extraction," p. 415, McGraw-Hill, New York (1952).
27. Smith, A. S., and T. B. Braun, *Ind. Eng. Chem.*, 37, 1048 (1954).
28. Stearn, A. E., and H. Eyring, *J. Phys. Chem.*, **44**, 955 (1940).
29. Treybal, R. E., "Liquid Extraction," p. 131, McGraw-Hill, New York (1951).
30. Wilke, C. R., *Chem. Eng. Progr.*, **46**, 95 (1950).
31. Wohl, Kurt, *Trans. Am. Inst. Chem. Engrs.*, **42**, 215 (1946); *Chem. Eng. Progr.*, **49**, 218 (1953).

Manuscript received December 2, 1960; revision received November 27, 1961; paper accepted November 29, 1961. Paper presented at A.I.Ch.E. New Orleans meeting.

Adsorption of Normal Paraffins and Sulfur Compounds on Activated Carbon

R. J. GRANT, MILTON MANES and S. B. SMITH

Pittsburgh Chemical Company, Pittsburgh, Pennsylvania

Adsorption isotherms on activated carbon were determined gravimetrically for normal C_1 and C_8-C_6 paraffins and subsequently for methyl, ethyl, and *n*-propyl mercaptans, hydrogen sulfide, carbonyl sulfide, and carbon disulfide, at pressures up to 1 atm. and from —23° to 100°C. Orthobaric liquid densities at low temperatures of some of the sulfur gases were determined pycnometrically. The adsorption data on correlation by the method of Lewis, Gilliland, Chertow, and Cadogan (*1*) gave two separate curves, one for the paraffins and one for the sulfur compounds. The results show the correlation to be useful for estimating the adsorptive capacity of chemically similar compounds from a minimum of experimental data.

The purpose of this work was to determine in detail the isotherms of individual normal paraffins on a single granular activated carbon adsorbent and, if possible, to correlate the isotherms by the method of Lewis, et al. (*1*). When isotherms of methane and *n*-butane were determined initially on a conventional volumetric adsorption apparatus and the results correlated, the *n*-butane isotherms diverged in the direction of lower capacity, in a manner similar to that previously noted by Walters (2). The effect observed could be explained by solubility of *n*-butane in the stopcock grease. A gravimetric adsorption apparatus with the McBain balance principle was therefore constructed; it gave consistent isotherms of methane and of propane to hexane. Subsequently for operating convenience a completely grease-free gravimetric system was constructed and used to determine the adsorption isotherms of a series of sulfur-containing compounds. The results were treated in the same fashion as the hydrocarbon data.

S. B. Smith is with A. D. Little, Inc., Cambridge, Massachusetts.

EXPERIMENTAL PROCEDURE

Apparatus

The McBain adsorption balance finally adopted was constructed of Pyrex pipe (adsorption chambers) and stainless steel

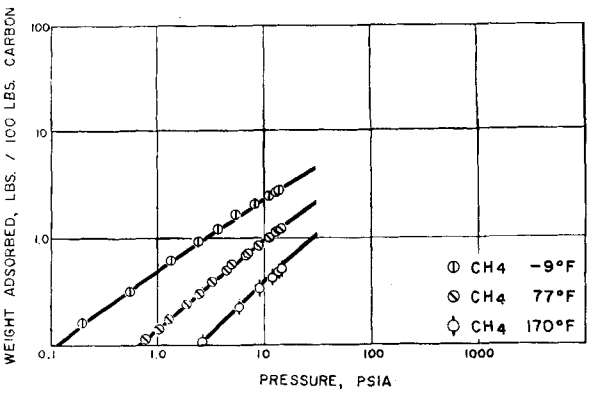

Fig. 1. Adsorption isotherms of methane on BPL (4 × 10) activated carbon.